Available online at www.sciencedirect.com
SCIENCE DIRECT
Polymer 47 (2006) 6167–6171
polymer
www.elsevier.com/locate/polymer

Natural microshells of alginate–chitosan: Unexpected stability and permeability

Xia Tao [a,*], Xue-Jun Sun [c], Jingmei Su [a], Jian-Feng Chen [b,*], Wilson Roa [c]

[a] Key Lab for Nanomaterials, Ministry of Education, Bei San Huan East Road 15, BUCT, Beijing 100029, PR China
[b] Research Center of the Ministry of Education for High Gravity Engineering & Technology, BUCT, Beijing 100029, PR China
[c] Cross Cancer Institute, University of Alberta, Canada T6G 1Z2

Received 19 April 2006; received in revised form 6 June 2006; accepted 11 June 2006
Available online 7 July 2006

Abstract

We utilized alginate sodium (ALG) and chitosan (CHI) as wall components to construct a natural and biodegradable polyelectrolyte microshell by the electrostatic self-assembly technique. The resultant ALG–CHI shells were found to maintain intact spherical shape in different poly(styrenesulfonate sodium) (PSS) bulk concentrations (maximal detection concentration 20.0 wt%). Compared with the shells composed of PSS and poly(allylamine hydrochloride) (PAH) that collapse or deform at a 4 wt% or more than 4 wt% PSS concentration, the ALG–CHI shells display higher stability. Meanwhile, the permeability of the ALG–CHI shells prior to and after incubation in PSS solutions was directly traced by the fluorescence recovery after photobleaching (FRAP). The composition of the ALG–CHI shells themselves is thought to be responsible for the differences in the stability.

Keywords: Alginate sodium; Chitosan; Permeability

1. Introduction

Layer-by-layer (LBL) self-assembly [1] of oppositely charged polyelectrolytes onto dissolvable colloidal particles has been utilized to create ultrathin microshells (microcapsules) with particular advantages, e.g., the tailored wall thickness on a nanometer-scale range, the ordered wall composition, as well as the controlled size and shape [2]. Both the preparation and behavior of such shells primarily composed of synthetic polyelectrolytes such as poly(styrenesulfonate sodium) (PSS) and poly(allylamine hydrochloride) (PAH) have been reported in much detail and reviewed [3]. For practical and biomedical applications, the use of polysaccharides instead of synthetic polyelectrolytes seems an attractive alternative.

Natural polysaccharides such as chitosan (CHI) and alginate sodium (ALG) have been widely investigated for applications in coating membranes, controlled-release drug delivery and biomaterials [4–6]. CHI is a natural cationic polymer derived from chitin *N*-deacetylation. ALG is an anionic polymer composed of a naturally occurring block copolymer of two monosaccharide units obtained from marine brown algae. The ALG–CHI polyelectrolyte complex (PEC) systems are commonly developed as a complex planar membrane and an ALG gel bead is coated with CHI [7–9], which places some limitations in controlling the membrane thickness on a nanometer-scale and characterizing the encapsulating PEC membrane precisely. Recently, we have constructed a natural and biocompatible polyelectrolyte microshell by using ALG and CHI as building blocks with the LBL self-assembly technique and investigated the photostability of the shells during the oxidative reaction, together with the accumulation ability of organic substances in aqueous solutions [10].

In the present study, the properties of the ALG–CHI shells were further studied and compared with the typical

* Corresponding authors. Tel.: +86 10 64448472; fax: +86 10 64434784.
E-mail addresses: taoxia@yahoo.com (X. Tao), chenjf@mail.buct.edu.cn (J.-F. Chen).

0032-3861/$ - see front matter © 2006 Elsevier Ltd. All rights reserved.
doi:10.1016/j.polymer.2006.06.038

polyelectrolyte shells made of PSS and PAH. Unexpectedly, the stability of the ALG–CHI shells in different media, e.g., PSS polyelectrolyte solutions with different concentrations was larger. Also, the permeability of the ALG–CHI shells prior to and after incubation in PSS solutions was directly traced by the fluorescence recovery after photobleaching (FRAP). The composition of the shells themselves is thought to be responsible for the differences in the stability.

2. Experimental section

2.1. Materials

ALG ($M_w = 12{,}000-80{,}000$) was obtained from Sigma, Canada. CHI ($M_w = 30{,}000$) was obtained from Primex Biochemicals, Norway. PSS ($M_w = 70{,}000$) and PAH ($M_w = 70{,}000$) were obtained from Aldrich. Melamine formaldehyde particles (MF particles) (4.89 ± 0.14 μm) were purchased from Microparticles GmbH, Germany. FITC-albumin and 6-carboxyfluorescein (6-CF) were purchased from Sigma. All chemicals were used as received. Millipore water was used throughout the study. For reference, the chemical structures of ALG and CHI are shown below.

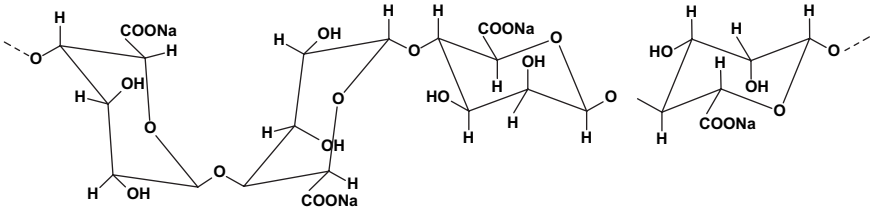

Alginate sodium (ALG)

Chitosan (CHI)

2.2. Preparation of shells and subsequent incubation in PSS solutions

Alginate sodium solution (1.5 ml) (1 mg/ml in 0.5 M NaCl) or 1.5 ml of chitosan solution (1 mg/ml in 0.2 M NaCl at pH 3.8), with a charge opposite to that of MF templates or the last layer deposited, was added to a template colloidal solution (0.3 ml), and was left to absorb for 1 h. The excess of added species was removed after each layer was deposited by three repeated centrifugation (2500 g, 3 min)/washing/redispersion cycles with dilute aqueous NaCl. Typically, five (ALG–CHI) bilayers were deposited. Hollow shells were obtained by dissolving the MF cores with HCl (0.16 M, 40 min), centrifuging (2500 g, 2 min) and washing three times with water.

Equal amounts of microshell suspension (aged for appropriate two days) and PSS solution of different concentrations were mixed together and incubated for 60 min.

2.3. Characterization

Confocal micrographs were taken with an LSM 510 confocal microscope (Carl Zeiss Inc.) equipped with multiple laser lines from UV to infrared for excitation of fluorophores. For FRAP measurements, the laser beam was focused onto a spot inside the whole shell. The interval between the image scans varied depending on the duration of the recovery. Recovery was considered complete when the intensity of the photobleached region stabilized.

SFM images were recorded at ambient temperature by using a Digital Instrument Nanoscopy IIIa in the tapping mode. Samples were prepared by applying a drop of the shell solution onto a freshly cleaved mica substrate. After the shells were allowed to settle, the substrate was extensively rinsed with Millipore water and then dried under a gentle stream of nitrogen.

3. Results and discussion

A method describing the stability of polyelectrolyte microshells has been built by CLSM studies on the deformation/rupture of the shells upon incubation in PSS polyelectrolyte solutions with different concentrations [11]. Fig. 1 shows CLSM images of hollow shells consisting of 10 layers of ALG–CHI in different PSS bulk concentrations after incubation for 60 min. A striking finding is that all the ALG–CHI shells maintain their spherical shape intact even when the PSS concentrations are increased upwards to 15.0 wt% (maximal detection concentration 20.0 wt%, not shown here). Compared with the PSS–PAH shells that collapse or deform at

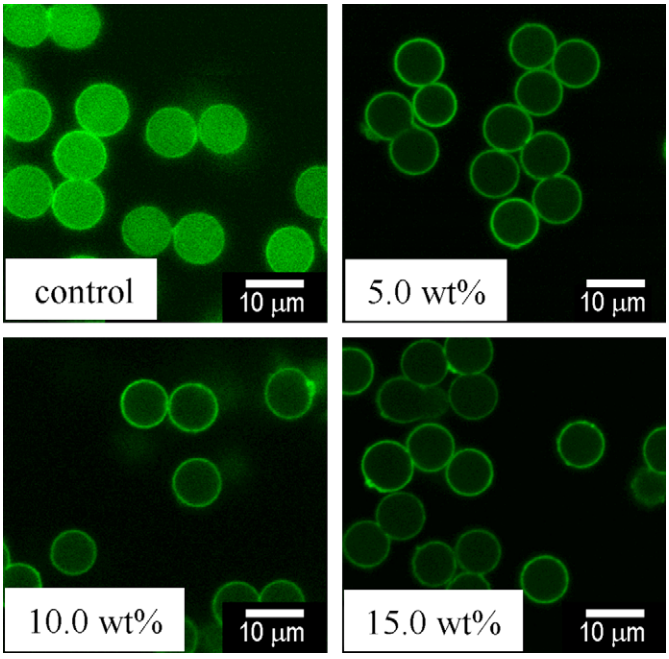

Fig. 1. CLSM images of hollow shells composed of $(ALG-CHI)_5$ as a function of the PSS ($M_w = 70{,}000$) bulk concentrations after incubation for 60 min. The PSS concentrations represented as wt% are indicated in the insets. FITC-albumin was used to label the shells. Fluorescence intensity from the interior of the shells can be eliminated by reducing the mixture time of a fluorescent label reagent and a microshell suspension.

a 4 wt% or more than 4 wt% PSS concentration [12,13], the ALG–CHI shells display more stability in the external media.

It has to be mentioned that in this study weakly cross-linked MF particles with an average diameter of 4.9 μm were chosen as removable templates, and that the resultant $(ALG-CHI)_5$ shells after removal of MF cores in HCl expanded to a large degree (ca. 8 μm in diameter, see control image in Fig. 1). Though for the moment we cannot provide reasonable explanation for the swollen shells, the cross-linked degree of MF particles themselves as well as the formation of the hydrogen bonds between the two polysaccharides, and the hydrogen bonds between the polysaccharides and water might be considered as possible reasons [4,7,14]. Further work is needed to proceed to investigate the detailed mechanism of the shell swelling.

To explore the shell structure changes before and after incubation in PSS solutions, the SFM technique can be employed [15]. Fig. 2a and b displays SFM images (top view) of the $(ALG-CHI)_5$ shells before and after incubation in 8.0 wt% PSS for 60 min. Apparently, the interior of the incubated shells is rather bright, indicating that PSS can cross the layer barrier of the shell wall, and accumulate inside the shells. Direct visualization in the above two cases was also provided by SFM measurements on surface plot of the shells. A non-incubated shell looks like a compressed plate (Fig. 2c), but an incubated shell looks like a small hill (Fig. 2d), also suggesting that a great deal of accumulation of PSS had occurred.

To further verify if the wall texture changes of the shells occurred upon incubating in PSS solutions, the ALG–CHI shells were followed directly under CLSM. The dye 6-CF was used as a probe. Fig. 3 shows typical FRAP measurements by CLSM. A closed region (region of interest, ROI) in the interior of the shells was chosen for the whole FRAP process. As one can see, the changes in fluorescence intensity of the closed region from top to bottom in two cases, i.e., prior to (Fig. 3a) and after (Fig. 3b) the incubation undergo three

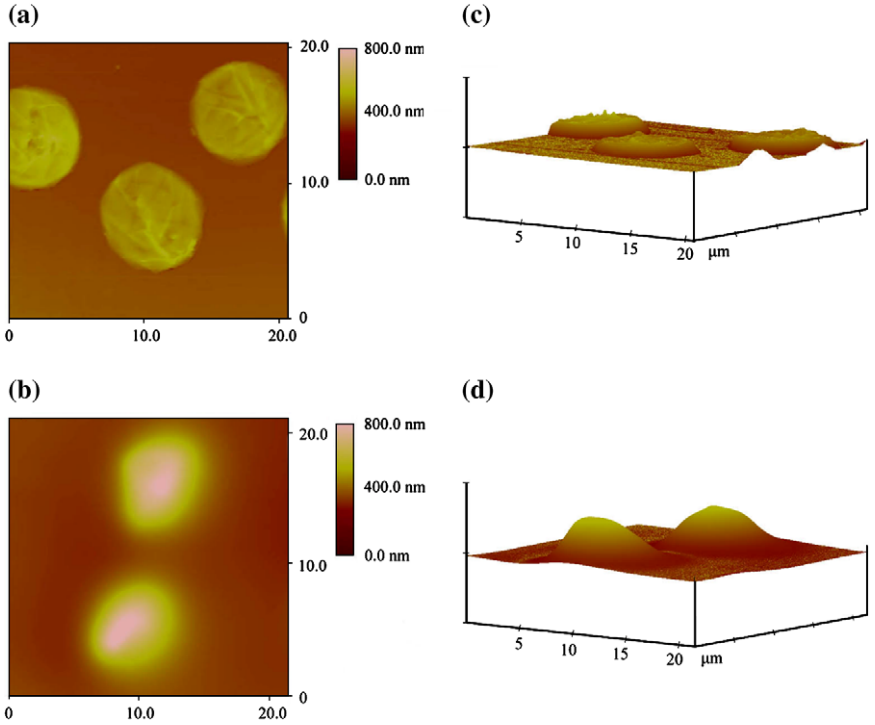

Fig. 2. SFM images of multilayer microshells of $(ALG-CHI)_5$ (a) before and (b) after incubation in 8.0 wt% PSS. Typical 3-D views corresponding to (a) and (b) are shown in (c) and (d).

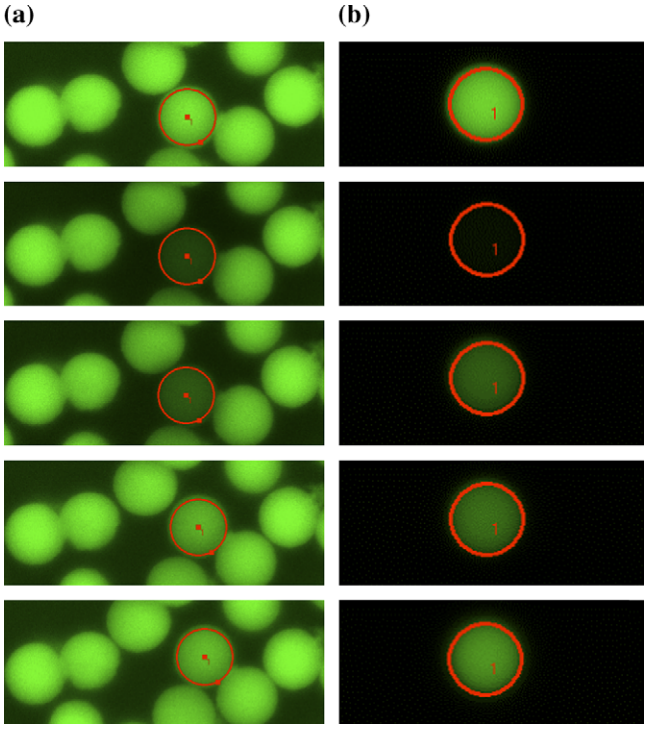

Fig. 3. Typical photochemical bleaching and recovery of the fluorescence of fluorescein in the interior of $(ALG–CHI)_5$ before (a) and after (b) incubation in 8.0 wt% PSS.

stages: (i) photochemical bleaching appearing as a dark center inside the shell; (ii) recovery of the bleached fluorescence from dark to strong; and (iii) stable fluorescence intensity in the shell interior.

Corresponding to Fig. 3, the fluorescence intensity in the shell interior after a bleach pulse as a function of time for shells coated with $(ALG–CHI)_5$ before and after incubation in PSS is shown in Fig. 4. From the figure, one can see that the fluorescence recovery time of the shells prior to incubation is ca. 700 s; while after the shells are incubated in 8 wt% PSS solution, the fluorescence recovery becomes only ca. 40 s, which indicates the formation of large holes in the walls.

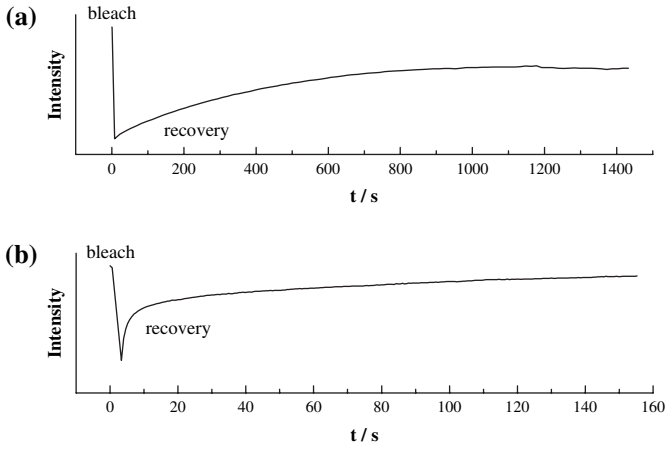

Fig. 4. The fluorescence intensity profile after a bleach pulse for $(ALG–CHI)_5$ shells before (a) and after (b) incubation in 8.0 wt% PSS.

Assuming the transport is diffusive across the wall of thickness $d \sim 43$ nm (obtained by SFM software analysis), the diffusion coefficient can be estimated according to a method mentioned in the literature [16], namely, $0.8 \times 10^{-12}\,cm^2\,s^{-1}$ for the non-incubated shells and $1.4 \times 10^{-11}\,cm^2\,s^{-1}$ for the incubated shells.

These results above demonstrated that the assembled shells made of ALG and CHI possess high stability in different PSS polyelectrolyte solutions. As a matter of fact, the shells are also rather stable and remain intact in spherical shape in other media, e.g., isothiocyanate-labeled PAH, fluorescein isothiocyanate-labeled albumin, and fluorescent-labeled polystyrene nanoparticles (28 nm in diameter) as well, as evidenced by CLSM measurements. Furthermore, these species can be accumulated inside the shells in more amounts. As previously reported [17], the species accumulated in the shells are more likely to be in an aggregated or complex form so that the real concentration within the interior of the microshells is lower than in the bulk solution, thus promoting accumulation (see Fig. 2). From these results we can speculate that different from the usual PSS–PAH shells that are impermeable for species with large molecular weight such as negatively charged albumin and nanoparticles, the ALG–CHI shells are permeable to various media. Thus, no deformation will be observed.

Compared with the PSS–PAH shells, the higher stability of the ALG–CHI shells should be attributed to the differences in their architecture. Alginate sodium is a straight-chain polysaccharide composed of two monomers, mannuronic acid and its C-5 epimer guluronic acid. Chitosan is a polysaccharide polymerized by *N*-acetyl-D-glucosamine and glucosamine. The ALG–CHI shells are obtained stepwise by the electrostatic interaction of the carboxylic groups of ALG chains and the amino groups of CHI, in which the cyclohexane rings are directly linked to the carboxylic groups of ALG chains and the amino groups of CHI. The cyclohexane rings themselves are more flexible than the methylene groups connected to the ammonium cations in PAH and the sulfonic acid anions in PSS because of their different arrangements and conformations in space. This is also in accord with a high elasticity, a larger degree of expansion during construction (see Fig. 1).

The enhanced permeability after incubation in PSS was ascribed to the rearrangement of the macromolecular layer constituents [13]. This situation originates from the external stimuli existent in the bulk solution, which might lead to a more porous scaffold with open porosity on the wall architecture. These dye molecules can enter into the produced pores, and then be in a different environment from those permeate into the ALG–CHI microshells. As a result, a different intensity recovery profile from ALG–CHI without PSS incubation may be anticipated (Fig. 4a).

4. Conclusions

The natural and biodegradable ALG–CHI hollow shell constructed via the self-assembly technique possesses good stability and elasticity. The unexpected higher stability of the ALG–CHI shells than the PSS–PAH shells in different

media can be explained as the result of the differences in their architecture. We expect that the shells may find wide utilities in the biomedical field and other applications.

Acknowledgements

The authors thank the National Natural Science Foundation of China (No. 20577002, 20546001 and 20325621) and Talent Program of BUCT for financial support.

References

[1] (a) Decher G. Fuzzy nanoassemblies: toward layered polymeric multicomposites. Science 1997;277:1232–7;
(b) Keller SW, Johnson SA, Brigham ES, Yonemoto EH, Mallouck TE. Photoinduced charge separation in multilayer thin films grown by sequential adsorption of polyelectrolytes. J Am Chem Soc 1995;117:12879–80;
(c) Ruths J, Essler F, Decher G, Riegler H. Polyelectrolytes I: polyanion/polycation multilayers at the air/monolayer/water interface as elements for quantitative polymer adsorption studies and preparation of heterosuperlattices on solid surfaces. Langmuir 2000;16:8871–8.

[2] Caruso F, Caruso R, Möhwald H. Nanoengineering of inorganic and hybrid hollow spheres by colloidal templating. Science 1998;282:1111–4.

[3] Peyratout CS, Dähne L. Tailor-made polyelectrolyte microcapsules: from multilayers to smart containers. Angew Chem Int Ed 2004;43:3762–83.

[4] (a) Miyazaki S, Nakayama A, Oda M, Takada M, Attwood D. Chitosan and sodium alginate based bioadhesive tables for intraoral drug delivery. Biol Pharm Bull 1994;17:745–7;
(b) Ravi Kumar MNV. Nano and microparticles as controlled drug delivery devices. J Pharm Pharmaceut Sci 2000;3:234–58.

[5] Yan XL, Khor E, Lim LY. Chitosan–alginate films prepared with chitosans of different molecular weights. J Biomed Mater Res 2001;58:358–65.

[6] (a) Rutnakornpituk M, Ngamdee P, Phinyocheep P. Synthesis, characterization and properties of chitosan modified with poly(ethylene glycol)–polydimethylsiloxane amphiphilic block copolymers. Polymer 2005;46:9742–52;
(b) Ye W, Leung MF, Kwong TL, Lee DKL, Li P. Novel core–shell particles with poly(*n*-butyl acrylate) cores and chitosan shells as an antibacterial coating for textiles. Polymer 2005;46:10538–43;
(c) Liu YL, Su YH, Lai Juin-Yih. In situ crosslinking of chitosan and formation of chitosan–silica hybrid membranes with using <gamma>-glycidoxypropyltrimethoxysilane as a crosslinking agent. Polymer 2004;45:6831–7.

[7] Wang L, Khor E, Lim LY. Chitosan–alginate–CaCl(2) system for membrane coat application. J Pharm Sci 2001;90:1134–42.

[8] Sezer AD, Akbuga J. Release characteristics of chitosan treated alginate beads: I. Sustained release of a macromolecular drug from chitosan treated alginate beads. J Microencapsul 1999;16:195–203.

[9] Takeuchi H, Yasuji T, Yamamoto H, Kawashima Y. Spray-dried lactose composite particles containing an ion complex of alginate–chitosan for designing a dry-coated tablet having a time-controlled releasing function. Pharm Res 2000;17:94–9.

[10] (a) Tao X, Su J, Chen J, Zhao J. A novel route for wastewater treatment: photo-assisted Fenton degradation of dye pollutants accumulated in natural polyelectrolyte microshells. Chem Commun 2005;4607–9;
(b) Tao X, Su J, Chen J. Photooxidative degradation of dye pollutants accumulated in self-assembled natural polyelectrolyte micro-shells under visible radiation. Chem Eur J 2006;12:4164–9.

[11] Vinogradova OI, Andrienko D, Lulevich VV, Nordschild S, Sukhorukov GB, Shackelford JF, et al. Young's modulus of polyelectrolyte multilayers from microcapsule swelling. Macromolecules 2004;37:1113–7.

[12] Cao C, Leporatti S, Moya S, Donath E, Möhwald H. Stability and mechanical properties of polyelectrolyte capsules obtained by stepwise assembly of poly(styrenesulfonate sodium salt) and poly(diallyldimethyl ammonium) chloride onto melamine resin particles. Langmuir 2001;17:3491–5.

[13] Dai Z, Dähne L, Möhwald H, Tiersch B. Novel capsules with high stability and controlled permeability by hierarchic templating. Angew Chem Int Ed 2002;41:4019–22.

[14] Lee KY, Mooney DJ. Hydrogels for tissue engineering. Chem Rev 2001;101:1869–79.

[15] (a) Matsumoto M, Miyazaki D, Tanaka M, Azumi R, Manda E, Kondo Y, et al. Reversible light-induced morphological change in Langmuir–Blodgett films. J Am Chem Soc 1998;120:1479–84;
(b) Gao C, Donath E, Moya S, Dudnik V, Möhwald H. Elasticity of hollow polyelectrolyte capsules prepared by the layer-by-layer technique. Eur Phys J E 2001;5:21–7;
(c) Gössl I, Shu L, Schlüter AD, Rabe JP. Molecular structure of single DNA complexes with positively charged dendronized polymers. J Am Chem Soc 2002;124:6860–5.

[16] Dai Z, Möhwald H. Highly stable and biocompatible nafion-based capsules with controlled permeability for low-molecular-weight species. Chem Eur J 2002;8:4751–5.

[17] Gao C, Donath E, Möhwald H, Shen J. Spontaneous deposition of water-soluble substances into microcapsules: phenomenon, mechanism, and applications. Angew Chem Int Ed 2002;41:3789–93.